A Brn2–Zic1 axis specifies the neuronal fate of retinoic-acid-treated embryonic stem cells

Sylvia Urban, Dominique Kobi, Marie Ennen, Diana Langer, Stéphanie Le Gras, Tao Ye, Irwin Davidson

© 2015. Published by The Company of Biologists Ltd | Journal of Cell Science (2015) 128, 2303-2318 doi:10.1242/jcs.168849

RESEARCH ARTICLE

A Brn2–Zic1 axis specifies the neuronal fate of retinoic-acid-treated embryonic stem cells

Sylvia Urban[1,*], Dominique Kobi[1,*], Marie Ennen[1], Diana Langer[1], Stéphanie Le Gras[1], Tao Ye[1] and Irwin Davidson[1,2,‡]

ABSTRACT

Mouse embryonic stem cells (ESCs) treated with all-trans retinoic acid differentiate into a homogenous population of glutamatergic neurons. Although differentiation is initiated through activation of target genes by the retinoic acid receptors, the downstream transcription factors specifying neuronal fate are less well characterised. Here, we show that the transcription factor Brn2 (also known as Pou3f2) is essential for the neuronal differentiation programme. By integrating results from RNA-seq following Brn2 silencing with results from Brn2 ChIP-seq, we identify a set of Brn2 target genes required for the neurogenic programme. Further integration of Brn2 ChIP-seq data from retinoic-acid-treated ESCs and P19 cells with data from ESCs differentiated into neuronal precursors by Fgf2 treatment and that from fibroblasts trans-differentiated into neurons by ectopic Brn2 expression showed that Brn2 occupied a distinct but overlapping set of genomic loci in these differing conditions. However, a set of common binding sites and target genes defined the core of the Brn2-regulated neuronal programme, among which was that encoding the transcription factor Zic1. Small hairpin RNA (shRNA)-mediated silencing of Zic1 prevented ESCs from differentiating into neuronal precursors, thus defining a hierarchical Brn2–Zic1 axis that is essential to specify neural fate in retinoic-acid-treated ESCs.

KEY WORDS: Ascl1, Fgf2, Sox2, ChIP-seq, Reprogramming

INTRODUCTION

Retinoic acid plays an essential role in embryonic development and in the homeostasis of many adult tissues (Niederreither and Dollé, 2008; Mark et al., 2006). Retinoic acid can be used to differentiate mouse embryonic stem cells (ESCs) into a highly homogenous population of glutamatergic neurons (Bibel et al., 2007, 2004; Götz and Barde, 2005) mimicking the generation of cortical glutamatergic neurons from Pax6-expressing progeny in the developing mouse cortex (Götz and Barde, 2005). The initial trigger for differentiation is the activation of target genes by the retinoic acid receptors (RARs), in particular the RARγ2 isoform (Al Tanoury et al., 2014). ESCs can also be differentiated into neuronal precursor cells by other techniques, such as by treatment with Fgf2 (Okabe et al., 1996; Wichterle et al., 2002).

Brn2 (also known as Pou3f2 or N-Oct3) is a Pou-homeodomain transcription factor with an important role in neurogenesis (Schonemann et al., 1998; Ryan and Rosenfeld, 1997). Brn2 is expressed in sub-ventricular zone progenitor cells throughout the neuraxis and, upon cell differentiation, is expressed in cortical layers II and III, and in V pyramidal neurons (Hagino-Yamagishi et al., 1997). *Brn2*-knockout neonates show neuronal loss only in the hypothalamic supraoptic and paraventricular nuclei, where the closely related *Brn1* (also known as *Pou3f3*) is not expressed (Nakai et al., 1995; Schonemann et al., 1995). In contrast, *Brn1* mutants display changes in brain morphology only in the hippocampus, which weakly expresses Brn2 (Sugitani et al., 2002). Both Brn1 and Brn2 are expressed and play redundant roles in the neocortex, where knockout of both Brn1 and Brn2 results in severe proliferation defects in cortical progenitor cells and migration defects in upper-layer neurons, ultimately leading to a disorganized and thinned cortex (McEvilly et al., 2002; Sugitani et al., 2002). In addition, Brn2 also plays an important role in Schwann cell development (Jaegle et al., 2003). The essential role of Brn2 in neurogenesis is highlighted by the fact that it can be used in combination with expression of Ascl1 and Mytl1 to reprogramme fibroblasts into a neuronal fate *in vitro* (Vierbuchen et al., 2010; Wapinski et al., 2013). Despite the crucial role of Brn2 in neurogenesis, its target genes and mode of action remain poorly characterised.

The Brn2 DNA-binding domain (DBD) consists of the POU-specific (POUs) and POU-homeodomain (POUh) domains connected by a flexible linker (Phillips and Luisi, 2000; Ryan and Rosenfeld, 1997). The POUs and POUh domains recognise DNA and provide sequence specificity (Cook and Sturm, 2008; Klemm et al., 1994). Brn2 can recognize several binding elements depending on the spacing and the positioning of the two subdomains (Klemm and Pabo, 1996). Brn2 binds as a dimer to at least three distinct types of sequence designated as palindromic Oct recognition elements (POREs), more palindromic Oct recognition elements (MOREs) and N-Oct-3 recognition elements (NOREs), as well as the simpler OCT motif (Alazard et al., 2005; Botquin et al., 1998; Millevoi et al., 2001; Nieto et al., 2007; Tomilin et al., 2000).

Although the initial events in retinoic-acid-induced differentiation have been well characterised (Mahony et al., 2011; Moutier et al., 2012; Al Tanoury et al., 2014), the downstream transcription factors required for specifying neural fate are unknown. Here, we show that Brn2 is essential for retinoic-acid-induced neuronal differentiation of ESCs. We identify a common set of Brn2-occupied sites and potential target genes that form the core of the Brn2-regulated neurogenesis network in different models of neuronal differentiation, and we identify transcription factor Zic1 as a crucial downstream target. Zic1 is essential for retinoic-acid-induced neuronal differentiation, and Brn2 and Zic1 cooperate to regulate a set of neurogenic genes. We thus identify a new Brn2–Zic1 axis as being essential for specifying the neuronal fate in retinoic-acid-treated ESCs.

[1]Department of Functional Genomics and Cancer, Institut de Génétique et de Biologie Moléculaire et Cellulaire, CNRS/INSERM/UDS, 1 Rue Laurent Fries, Illkirch, Cédex 67404, France. [2]Equipe Labellisée of the Ligue Nationale Contre le Cancer, CNRS/INSERM/UDS, 1 Rue Laurent Fries, Illkirch, Cédex 67404, France.
*These authors contributed equally to this work

‡Author for correspondence (irwin@igbmc.fr)

Received 13 January 2015; Accepted 13 May 2015

Journal of Cell Science

Journal of Cell Science (2015) 128, 2303-2318 doi:10.1242/jcs.168849

RESULTS

BRN2 is essential for the neuronal identity of retinoic-acid-differentiated embryoid bodies

Treatment of ESCs grown as embryoid bodies with retinoic acid induces a large set of genes and triggers a developmental programme leading to their differentiation as glutamatergic neurons (Fig. 1A) (Bibel et al., 2007; Moutier et al., 2012). Examination of the RNA-seq data and quantitative reverse-transcription PCR (RT-qPCR) analysis identified several transcription factors whose expression was induced at various times after retinoic acid treatment (supplementary material Fig. S1A). Retinoic acid treatment repressed expression of *Pou5f1* (also known as *Oct4*) and *Nanog*, but had less effect on that of *Sox2*, which continued to be expressed at later stages of differentiation. Expression of *Pax6*, *Pax3*, nestin (*Nes*) and *Mapt* were clearly detectable at 24–48 h after retinoic acid addition (supplementary material Fig. S1A), whereas *Ascl1*, *Msx3*, *Dcx1* and *Pou3f2* (supplementary material Fig. S1A) were evident only later, at between 48 and 96 h. Several of these factors are involved in diverse aspects of neurogenesis *in vivo* (see, for example, Castro and Guillemot, 2011; Ramos and Robert, 2005). In particular, Brn2 mRNA and protein were strongly expressed only at 72–96 h after retinoic acid treatment, which is during the time that neuronal precursors are specified and after the initiation of Zic1 expression (Fig. 1B,C, and see below).

To test the requirement of Brn2 in retinoic-acid-induced neuronal differentiation of embryoid bodies, we used lentivirus vectors expressing a small hairpin RNA (shRNA) directed against Brn2 (ShBrn2) or a control shRNA (ShC) to infect ESCs subsequently selected with puromycin and differentiated as retinoic-acid-treated embryoid bodies. Knockdown of Brn2 expression after 96 h of retinoic acid treatment could be seen both by RT-qPCR and immunoblotting (Fig. 1D,E). Brn2 silencing led to a marked reduction in the number of surviving neuronal cells at 24 h after embryoid body dissociation (Fig. 1F). Surviving cells did not show the typical morphology of early neurons as they had only a few long axonal projections and a diminished number of cells with rounded and refringent cell bodies. Staining of ShC cells with Tubb3 (also known as Tuj1) showed that there was neuronal differentiation and an abundant Tubb3-stained axonal network, whereas in ShBrn2 cells, although a few Tubb3-stained cells were observed, there was no axonal network (Fig. 1G). Staining with antibody against Brn2 showed its presence in both the nucleus and cytoplasm of the ShC cells, whereas only weak staining was seen in the ShBrn2 cells. We also performed immunofluorescence with antibodies against Pax6, which strongly stained most nuclei of the ShC cell group (supplementary material Fig. S1B). In the Brn2-knockdown cells, Pax6 labelling was more heterogeneous, with some strong staining cells, but with many cells showing lower staining. In addition, the knockdown cells died after 2–3 days in culture, indicating that they do not survive in the medium and plating conditions that favour neuronal cells (data not shown).

ShBrn2 knockdown led to diminished expression of several neuronal marker genes normally induced in wild-type (WT) ESCs (Fig. 1H). RNA-seq on the embryoid bodies from ShBrn2 and shC infections treated with retinoic acid for 96 h identified ∼280 downregulated genes and 275 upregulated genes (supplementary material Table S1). Downregulated genes were enriched in ontology terms such as neurogenesis and transcription regulation (supplementary material Fig. S2A,B; Table S2), and included crucial regulators of neurogenesis, such as *Ascl1*, *Neurog1*, *Dcx*, *Dcc*, *Zic1*, *Zic2*, *Zic4*, *Zic5*, *Slit1* and *Uncx*. Brn2 silencing affected Notch signalling because expression of *Dll1*, *Dll3* and *Jag1* and the downstream targets *Hes3* and *Hes5* were all diminished (supplementary material Fig. S2B). In contrast, upregulated genes were associated with terms such as interferon-mediated immunity and mesoderm development (supplementary material Fig. S2A,B). Brn2 is therefore an upstream regulator of a network specifying neuronal identity of differentiating ESCs. In the absence of Brn2, surviving cells showed a loss of the axonal network, reduced expression of many neurogenic genes and, instead, expressed a diverse set of genes associated with mesoderm and endoderm differentiation and showed upregulated expression of *Foxd1*, a marker for reprogramming of cell fate (Koga et al., 2014). These cells also show a more general defect characterised by the activation of the interferon response.

Brn2 directly regulates genes that are crucial for neuronal differentiation

To identify genes directly regulated by Brn2, we performed ChIP-seq profiling of its genome occupancy in embryoid bodies treated with retinoic acid for 96 h and identified >2100 occupied sites, which although being in both inter- and intra-genic regions, were strongly enriched in promoter regions (−1 kb to +100 bp) compared to the representation of this region in the genome (Fig. 2A; supplementary material Table S3). In agreement with this, Brn2-occupied sites were enriched around the transcription start site (TSS) (Fig. 2B). Brn2-occupied sites were found at the *Neurog1*, *Pou6f1* and *Epha10* loci (Fig. 2C).

Brn2 binds recognition motifs such as the NOREs, MOREs and POREs, as well as the simpler OCT motif. We found few OCT motifs that fully matched the consensus at Brn2-occupied sites, but many sites with a single mismatch were observed (Fig. 2D). Similarly, only a few consensus NORE motifs were identified, but upon allowing a single mismatch up to 266 motifs were found. However, this motif is rather degenerate and allowing an additional mismatch leads to a very loose consensus meaning the significance of these sites is uncertain. No PORE motifs were found. Instead, the most frequent motif was the MORE with 143 consensus elements and up to 459 with a single mismatch. MORE+1 motifs with a single base pair insertion between the palindromic pseudo-repeats were also strongly represented in the Brn2-bound sequences. Similarly, MORE and MORE+1 sequences were among the most significantly enriched motifs found in a *de novo* MEME motif discovery analysis of 600 Brn2-occupied sites. These motifs were centred under the binding peaks, which is consistent with them acting as the Brn2-binding site (Fig. 2E), confirming that MORE and MORE+1 are the most represented motifs in retinoic-acid-treated embryoid bodies. Note that an OCT motif with a single mismatch is also contained within the MORE sites and thus many of the detected OCT elements overlap with the MOREs.

MEME analysis also revealed enrichment of a ZFX-like binding motif in the Brn2-occupied regions. This motif was more abundant than the MORE or MORE+1 elements, but was not located at the centre of the binding sites (Fig. 2E), being rather located flanking the MORE motifs. Brn2 sites with ZFX-like motifs were strongly enriched at the proximal promoter TSS, but were rarer at distal sites (supplementary material Fig. S2C). We examined the association between the Brn2-bound motifs and those of other transcription factors. Motif co-occurrence analysis (Fig. 2F) revealed an enriched association between the MORE or MORE+1 sites and motifs for various factors, such Meis transcription factors, which are important in neurogenesis (Agoston et al., 2014; Yamada et al., 2013), the DR1 motif for the Rar–Rxr or Pparg–Rxr heterodimers, and Runx1 and Foxd3. There is, however, selectivity as MORE sites associate with motifs for other nuclear receptors, notably the DR5 for Rar–Rxr, and

Journal of Cell Science (2015) 128, 2303-2318 doi:10.1242/jcs.168849

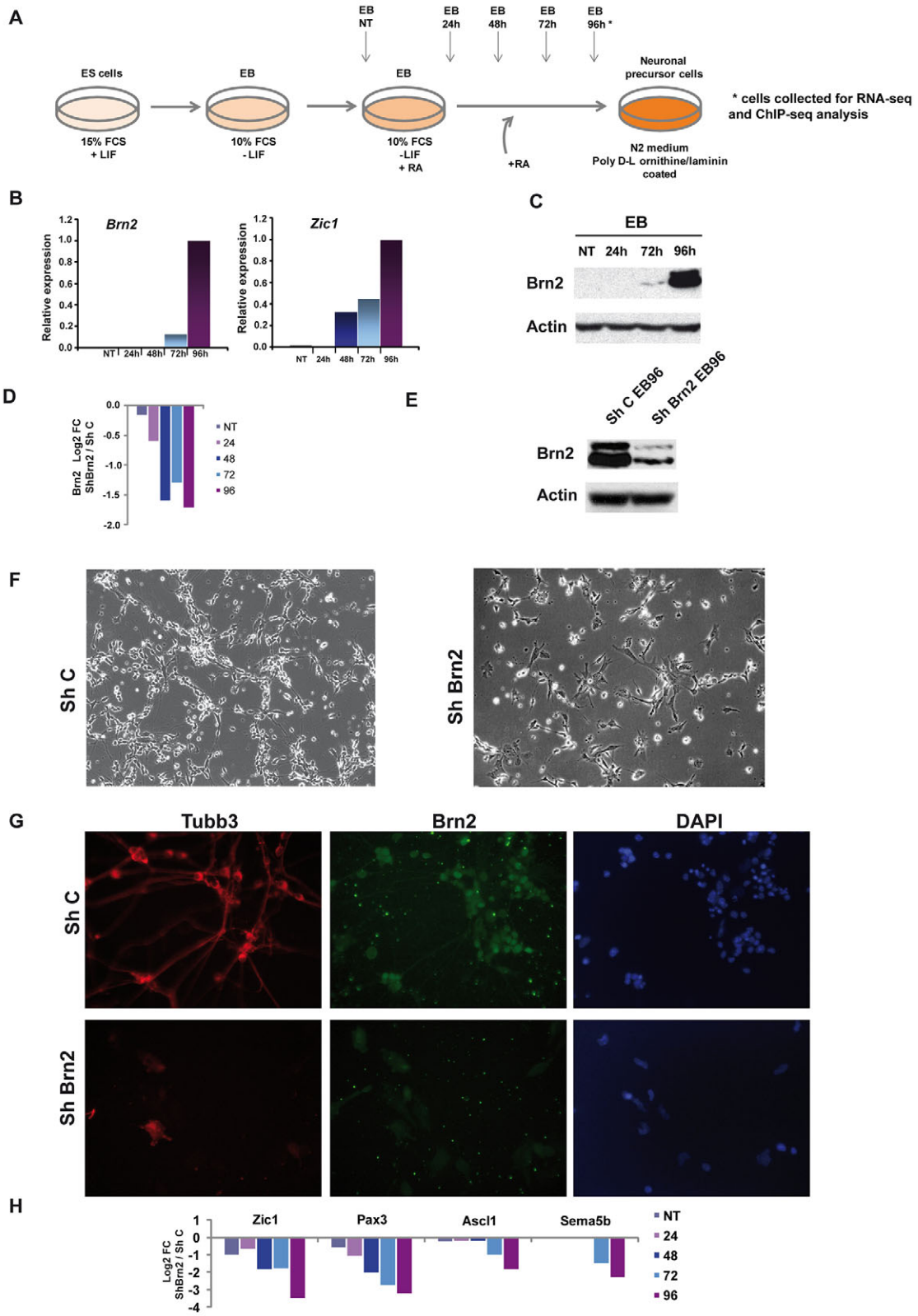

Fig. 1. Brn2 is required for neuronal differentiation of retinoic acid-treated embryoid bodies. (A) The protocol for neuronal differentiation of mouse ESCs is schematised. EB, embryoid bodies; RA, retinoic acid; NT, not treated with retinoic acid. (B) Brn2 and Zic1 expression in retinoic-acid-treated embryoid bodies was measured by RT-qPCR. (C) Brn2 expression in retinoic-acid-treated embryoid bodies was measured by immunoblotting. (D,E) The downregulated expression of Brn2 upon expression of ShBrn2 was measured by RT-qPCR (D) and by immunoblotting (E). FC, fold change. (F) Phase contrast microscopy images of cells expressing the indicated shRNAs 24 h after dissociation of the embryoid bodies. Images were taken at 20× magnification. (G) Immunofluoresence was performed on shC and shBrn2 cells with antibodies against Tubb3 and Brn2 as indicated and counterstained with DAPI. Note that these cells represent an independent experiment from F. (H) The relative expression of the indicated genes in shBrn2 and shC cells was measured by RT-qPCR at the indicated times. Quantitative results show the mean of three experiments.

Journal of Cell Science

Journal of Cell Science (2015) 128, 2303-2318 doi:10.1242/jcs.168849

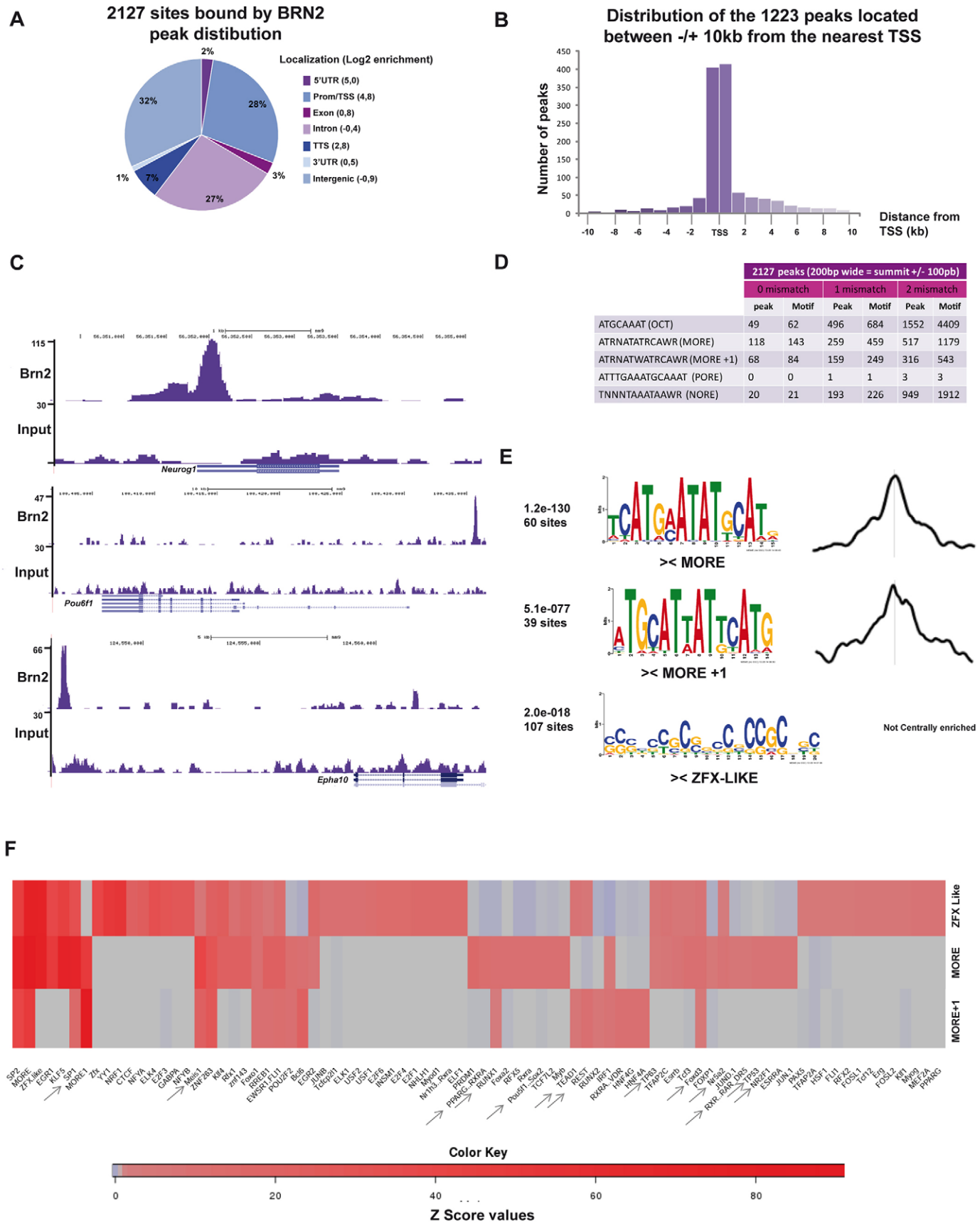

Fig. 2. See next page for legend.

Journal of Cell Science (2015) 128, 2303-2318 doi:10.1242/jcs.168849

Fig. 2. Genome occupancy of Brn2 in retinoic-acid-treated embryoid bodies. (A) Pie-chart showing the genomic distribution of Brn2-bound sites and their enrichment in the promoter region. (B) Brn2-bound sites are enriched around the TSS. The graph shows a plot of the frequency of Brn2-occupied sites versus the distance to TSS. (C) University of California at Santa Cruz genome browser screenshots of the indicated loci illustrating representative Brn2-binding sites. (D) Table indicating the frequency of occurrence of the indicated sequence motifs at the Brn2-occupied sites. (E) Analysis of the sequences at 600 Brn2-binding sites using MEME-ChIP identifies the MORE and MORE+1 motifs as the two most enriched motifs centred over the peak. A more degenerate Zfx-like motif was also detected. (F) The co-occurrence of transcription-factor-binding motifs with MORE and MORE+1 at Brn2-occupied sites is represented as a heatmap matrix. Arrows indicate motifs for several transcription factors that are relevant for neurogenesis.

sites for Nr5a2 and Nr2f1 (Coup-Tf1), as well as for Trp53 and Trp63, whereas MORE+1 sites are associated with motifs targeted by Tead1 and Rest, both of which have known functions in neurogenesis (Ballas and Mandel, 2005; Cao et al., 2008). Brn2 might therefore cooperate with these factors and factors binding the ZFX-like motif to regulate expression of neurogenic genes.

Integrating the RNA-seq and ChIP-seq data identified genes associated with Brn2-occupied sites and altered expression. Using a window of ±40 kb with respect to the binding peak, 2616 genes were associated with Brn2-bound sites (supplementary material Fig. S2D), and these were strongly enriched in functions like mRNA transcription, cell cycle and neurogenesis (supplementary material Fig. S2E,F). Nevertheless, of these, only 36 showed diminished expression upon Brn2 silencing, and 13 showed upregulation (supplementary material Fig. S2D,G). Among the directly downregulated targets were genes coding for transcription factors, such as Ascl1 and Neurog1, the neurogenic POU-factor Pou6f1, and Zic1 and Zic4. These 36 genes were associated with 48 Brn2-occupied sites enriched around the TSS (supplementary material Fig. S2H), and a majority were associated with MORE or MORE+1 motifs. In contrast, only 13 upregulated genes were associated with Brn2-bound sites and these showed no specific preference for their location relative to the TSS. These data are consistent with the idea that Brn2 directly activates expression of neurogenic transcription factors that in turn regulate other genes to promote neuronal differentiation.

We also performed Brn2 gain-of-function experiments to identify additional potential target genes. We infected ESCs with a lentivirus vector where Brn2 expression is under the control of 3×DR5 retinoic-acid-response elements. Ectopic Brn2 expression controlled by retinoic acid was induced prematurely 24 h after retinoic acid treatment and persisted over 96 h (Fig. 3A,B). Brn2 overexpression had little effect on the number of neurons and their morphology (data not shown), but enhanced expression of several of its target genes was seen. Interestingly, although Brn2 was prematurely expressed by 24 h, an overexpression of its target genes was only observed at 96 h (Fig. 3C).

RNA-seq analysis from embryoid bodies prematurely expressing ectopic Brn2 showed that 393 genes were upregulated and 327 were downregulated (supplementary material Table S1). Premature Brn2 expression enhanced expression of neurogenic genes (Fig. 3D, supplementary material Table S2), among which were *Dcx*, *Dcc*, *Mapt*, *Slit1*, *Zic1*, *Zic2*, *Zic4* and *Zic5*, as well as several other Pou domain factors (*Pou2f2*, *Pou4f1* and *Pou6f1*). Genes downregulated by premature Brn2 expression were notably enriched in mesoderm factors (Fig. 3E), like *Nkx2-1*, *Nkx6-1*, *Nkx6-2* and *Gata3*. Thus, premature gain of Brn2 function promotes expression of neurogenesis genes and neural fate while repressing other fates.

Comparison of deregulated genes in Brn2 loss- and gain-of-function experiments showed that there was a substantial overlap. Only three genes were up-regulated in both the gain- and loss-of-function experiments and none were downregulated (data not shown), whereas 134 (47%) genes downregulated by loss of Brn2 were upregulated after Brn2 overexpression (Fig. 3F). Similarly, 47 (17%) genes upregulated after loss of Brn2 were downregulated by overexpression (Fig. 3G). Integration with ChIP-seq data showed that 44 of the 393 genes whose expression was induced by Brn2 overexpression were associated with a Brn2-binding site (Fig. 3H,I). Of the 134 genes that were induced by gain of function and repressed by loss of function, 15 were associated with Brn2-occupied sites, but only 2 of the 47 genes that appeared as repressed by Brn2 were associated with such sites (Fig. 3J). These results compliment those seen upon Brn2 knockdown, defining a larger set of genes regulated both directly and indirectly by Brn2 during differentiation.

Comparison of Brn2 genomic localisation in ESCs induced to differentiate into neurons by different pathways

ESCs can be induced to differentiate into neurons by other protocols. Lodato et al. have analysed Brn2 genomic occupancy in ESCs induced to differentiate into neural progenitor cells (NPCs) after withdrawal of Fgf2 (Lodato et al., 2013). They identified many Sox2- and Brn2-bound sites at active H3K27ac-marked enhancer elements for genes involved in neuronal differentiation.

To facilitate comparison with the data presented here in retinoic-acid-induced embryoid bodies, we re-analysed the data from Fgf2-induced NPCs with the same criteria in the MACS programme used to analyse our data and considered only peaks called in both of their replicate samples to obtain a stringent set of peaks. Lodato et al. reported 6574 Brn2-occupied sites in Fgf2-induced NPCs (Lodato et al., 2013). Our re-analysis, identified only 3005 peaks in the more stringent set (supplementary material Fig. S3A), of which only 323 (i.e. ∼10%) are common to both the Lodato and our data sets (supplementary material Fig. S3B). Similarly, we analysed a second data set in which Brn2 was overexpressed in a Tet0-inducible manner (Lodato et al., 2013). Re-analysis of this data, from Brn2 ChIP in the control line without ectopic Brn2, identified 2031 peaks, compared to the 8400 reported by Lodato et al., of which 303 were also occupied in retinoic-acid-induced embryoid bodies (supplementary material Fig. S3A,B). Re-analysis using the input data set from the ectopic expressing line identified only 1541 peaks of which 286 were occupied in retinoic-acid-induced embryoid bodies. Moreover, there was limited overlap between Brn2 sites in Fgf2-induced NPCs and following ectopic expression, as only 202 (200 using the input as control for the Tet0 data) sites were occupied under all conditions.

Analysis of Brn2-bound peaks in the Fgf2-induced NPCs revealed an enrichment in degenerate MORE motifs (supplementary material Fig. S3C) similar to in the TetO dataset. An additional OCT motif was, however, found in the TetO dataset (supplementary material Fig. S3D). The 202 sites that were occupied under all conditions were strongly enriched in MORE-type motifs, similar to the retinoic-acid-induced embryoid bodies (supplementary material Fig. S3E).

Lodato et al. reported an association between Brn2- and Sox2-occupied sites. Re-analysis of the Sox2 ChIP-seq data set identified 10,207 sites compared to the 16,685 previously reported, and we clearly detected the Sox2 consensus motif at these sites (supplementary material Fig. S3A,F). Nevertheless, although there was a significant overlap between the Brn2 and Sox2 sites in the Fgf2-induced NPC data, there was little overlap with sites occupied by ectopic TetO-induced Brn2 and only 43 sites shared with Sox2 were seen when combining both data sets (supplementary material Fig. S3G).

Journal of Cell Science (2015) 128, 2303-2318 doi:10.1242/jcs.168849

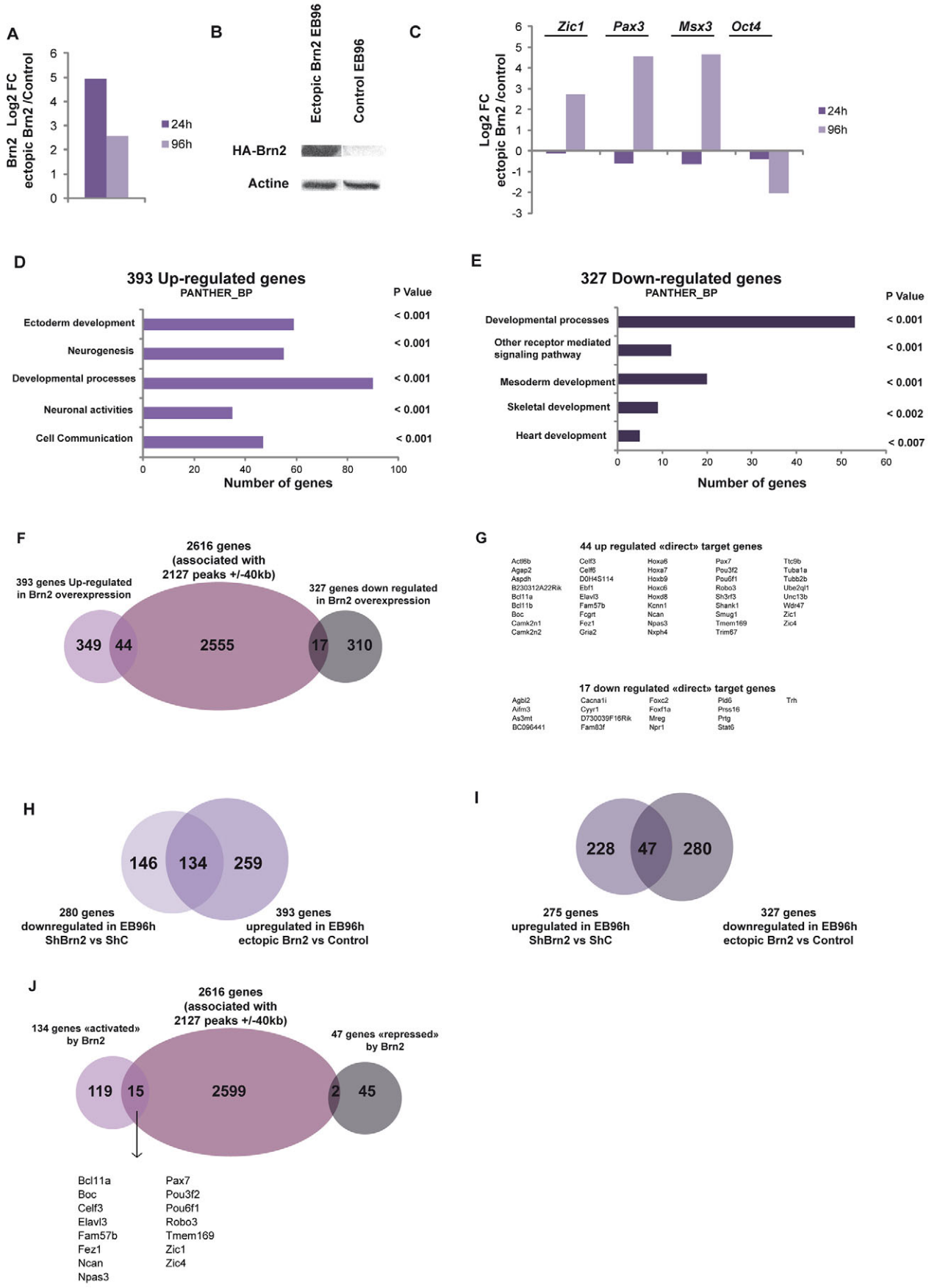

Fig. 3. See next page for legend.

Journal of Cell Science (2015) 128, 2303-2318 doi:10.1242/jcs.168849

Fig. 3. Gain of Brn2 function identifies additional target genes. (A,B) RT-qPCR (A) and anti-HA western blot analysis (B) shows Brn2 overexpression in retinoic-acid-treated embryoid bodies at the indicated times. EB, embryoid bodies; RA, retinoic acid; NT, not treated with retinoic acid. (C) RT-qPCR shows increased expression of Brn2 target genes upon gain of function and stronger repression of Oct4 (also known as POU5F1) expression. Results in A and C show the mean of three experiments. FC, fold change. (D,E) Ontology analysis of genes showing enhanced activation or repression upon Brn2 gain of function. (F,G) Numbers and names of genes showing complementary expression profiles upon loss and gain of Brn2. (H) Comparison of RNA-seq and ChIP-seq data identifies additional genes up- or down-regulated by Brn2 gain of function that are associated with Brn2-occupied sites. (I) List of genes that are potential direct targets identified in H. (J) Identification of 15 genes that show complimentary expression patterns in Brn2 loss- and gain-of-function experiments and association with Brn2-occupied sites.

As Lodato et al. reported that Brn2 and Sox2 associated with active H3K27ac-marked enhancers, we examined whether Brn2 sites in retinoic-acid-induced embryoid bodies and that were also occupied in NPCs were enriched at active H3K27ac-marked enhancer elements. We performed H3K27ac ChIP-seq in embryoid bodies treated with retinoic acid for 96 h and annotated 72,325 H3K27ac regions of which 59,800 were classed as distal enhancers using the using the criteria of Lodato et al. (i.e. >1 kb from the TSS). Of the 2127 Brn2 sites, 1295 were associated with H3K27ac-marked regions, of which 486 were at distal enhancers and 809 at promoters (<1 kb from TSS) (supplementary material Fig. S3H). A majority of Brn2 sites are therefore associated with active H3K27ac-marked regions in embryoid bodies.

Taken together, these data show that Brn2 occupies a distinct set of target sites in Fgf2- and retinoic-acid-induced embryoid bodies. Although there is an association of Brn2 sites with Sox2 sites in Fgf2-induced NPCs, this is not seen in retinoic-acid-induced embryoid bodies or at sites shared between the two cell models. We identified a shared set of sites highly enriched in MORE-type motifs and associated with genes essential for neuronal differentiation.

Brn2 is essential for P19 cell neuronal differentiation

We extended our study to P19 embryonic carcinoma cells as an additional model for neuronal differentiation. P19 cells differentiate into a diverse set of neurons when grow as retinoic-acid-treated aggregates for 4 days before plating in neuronal-specific medium (Fig. 4A). Brn2 expression was strongly induced 24 h after retinoic acid treatment and persisted in the aggregates throughout the 4 days of the experiment (Fig. 4B,C). We silenced Brn2 expression by lentiviral infection and differentiated the infected cell population. Brn2 expression was strongly repressed after 4 days of retinoic acid treatment (Fig. 4D,E), and the resulting cell population failed to differentiate into typical neuronal-like cells (Fig. 4F). Brn2 therefore promotes retinoic-acid-induced neuronal differentiation of both ESCs and P19 cells (see also Fujii and Hamada, 1993). We also generated cells constitutively expressing ectopic Brn2 to determine whether its expression could bypass the requirement for retinoic acid treatment. However, no neuronal differentiation could be seen in absence of retinoic acid showing that Brn2 is necessary, but not sufficient, for differentiation (data not shown).

Expression of many neuronal markers was repressed in the Brn2-silenced P19 cells (Fig. 4G). Further RNA-seq analysis, after plating as neurons, identified 1653 downregulated genes (supplementary material Table S1) that were strongly enriched in neuronal markers (Fig. 4H and supplementary material Table S2). More than 1500 upregulated genes were identified, and this group contained numerous genes associated with mesoderm development, including several bone morphogenetic proteins (BMPs), among which Bmp4 plays an important role in embryonic mesoderm formation (Hogan, 1996) (Fig. 4I; supplementary material Table S2). Of the 280 genes downregulated by *Brn2* silencing in retinoic-acid-induced embryoid bodies, 195 were also downregulated in P19 cells (supplementary material Fig. S4A). Thus, despite the differences between these two model systems, Brn2 regulates many of the same genes in both cell lines. The larger number of regulated genes in the P19 cells probably reflects the fact that these were analysed 4 days after induction of Brn2 expression in re-plated neurons, whereas in the retinoic-acid-induced embryoid bodies, we analysed gene expression only 24–48 h after Brn2 expression appeared. The shared genes therefore likely correspond to the initial Brn2-induced gene expression programme. Of the 275 genes upregulated by shBrn2 silencing, only 67 were upregulated in P19 cells and they were enriched in terms associated with interferon-mediated immunity (supplementary material Fig. S4B).

To identify Brn2 target genes in P19 cells, we performed ChIP-seq in retinoic-acid-treated P19 aggregates. However, expression of Brn2 after 4 days of retinoic acid induction was significantly lower in P19 cells (Agg4) compared to retinoic-acid-treated embryoid bodies (supplementary material Fig. S4C), and we were unsuccessful in obtaining a meaningful ChIP-seq profile. We engineered P19 cells to express ectopic Brn2 under the control of 3×DR5 elements such that its expression was induced by retinoic acid at the same time as the endogenous protein. We performed ChIP-seq 24 h after retinoic acid treatment to identify the first set of genes bound and potentially regulated by Brn2, identifying 1743 occupied sites (supplementary material Fig. S4D,E and Table S3). Brn2-occupied sites in P19 cells showed no enrichment at the promoter, but were located at distal inter- and intra-genic regions (supplementary material Fig. S4D) and comprised a few NORE motifs, but mostly MORE and MORE+1 and OCT motifs (supplementary material Fig. S4F). MEME analysis also identified a MORE-type motif centred beneath the peaks as the most enriched sequence (supplementary material Fig. S4G). Thus, like in retinoic-acid-induced embryoid bodies, Brn2 preferentially occupies MORE-like motifs in P19 cells.

We also compared ectopic Brn2 occupancy with genes that are downregulated in shBrn2-expressing cells. Using a window of ±40 kb with respect to the peak, 673 genes were associated with the 1743 Brn2-occupied sites (supplementary material Fig. S4H). Of these, 100 were downregulated upon Brn2 silencing, whereas 49 were among the upregulated genes. Even if this analysis is of limited value, given that we compared Brn2 occupancy at 24 h with RNA-seq in plated neurons 5 days later, we could still identify 100 genes, among which were *Neurog1*, *Zic1* and *Zic4* previously identified in retinoic-acid-induced embryoid bodies (supplementary material Fig. S4I). Moreover, as we performed the ChIP-seq analysis after 24 h, it is likely that these genes represent the first to be bound and activated by Brn2 following its induction by retinoic acid treatment.

Comparison of Brn2 occupancy in P19 cells and retinoic-acid-induced embryoid bodies identified 287 common binding sites (Fig. 5A,B) that were enriched in one or several MORE and MORE+1 motifs (Fig. 5C). These common sites are associated with 202 potential target genes enriched in neurogenesis functions (Fig. 5D) of which 10 are both downregulated upon Brn2 silencing in retinoic-acid-induced embryoid bodies and P19 cells (Fig. 5E). Among these are *Neurog1*, *Pou6f1*, *Zic1* and *Zic4*. Brn2 therefore occupies a distinct set of sites in the two cell types, but the common sites comprise MORE-type motifs and are associated with a small number of neurogenesis genes that define an early-induced gene expression programme common to both cell types.

Journal of Cell Science (2015) 128, 2303-2318 doi:10.1242/jcs.168849

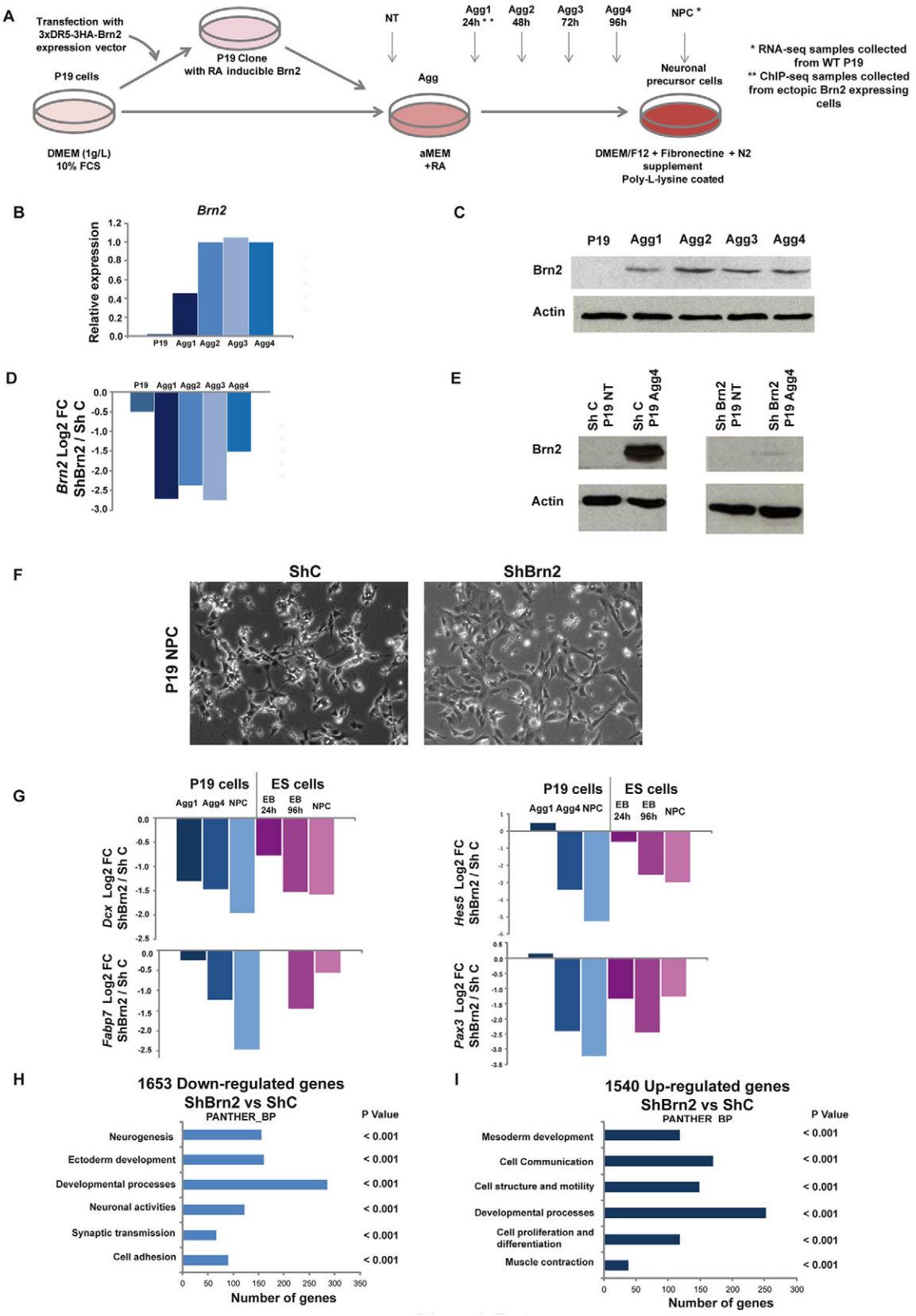

Fig. 4. Brn2 is required for retinoic acid-induced neuronal differentiation of P19 cells. (A) The differentiation protocol for P19 cells is schematised. Agg, aggregate; NT, not treated with retinoic acid. (B,C) RT-qPCR and western blot analysis of Brn2 expression during P19 cell differentiation. (D,E) RT-qPCR and western blot analysis of showing reduced Brn2 expression in P19 cells expressing shRNA. FC, fold change. (F) Phase contrast microscopy images of P19 cells expressing the indicated shRNAs 24 h after dissociation of aggregates. Images were taken at 20× magnification. (G) Comparative gene expression in differentiating P19 cells and embryoid bodies (EB) following shBrn2 knockdown. (H,I) Ontology analysis of genes whose expression was up- or down-regulated following Brn2 knockdown.

Journal of Cell Science (2015) 128, 2303-2318 doi:10.1242/jcs.168849

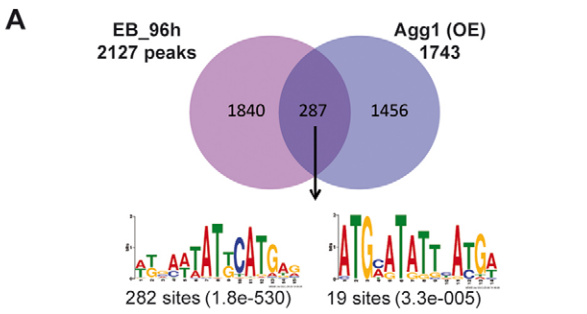

C

	MORE	MORE+1	Both
EB 96h (2127)	287 (13.5%)	215 (10.1%)	44 (2.1%)
Agg1 OE (1743)	671 (38.5%)	684 (39.2%)	108 (6.2%)
Common (287)	159 (55.4%)	137 (47.7%)	27 (9.4%)

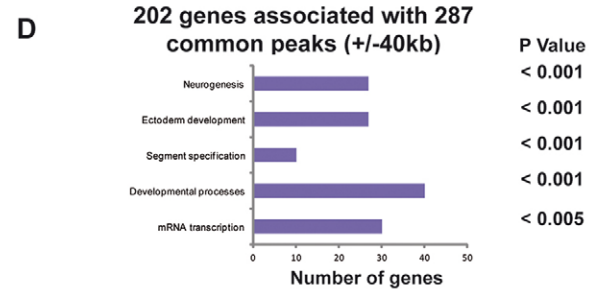

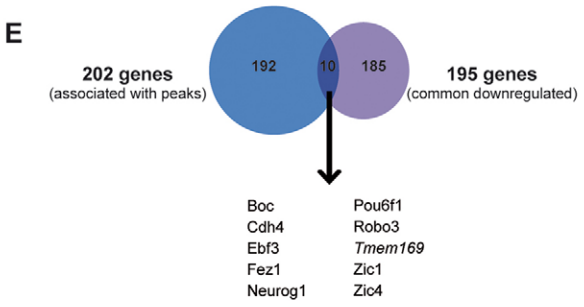

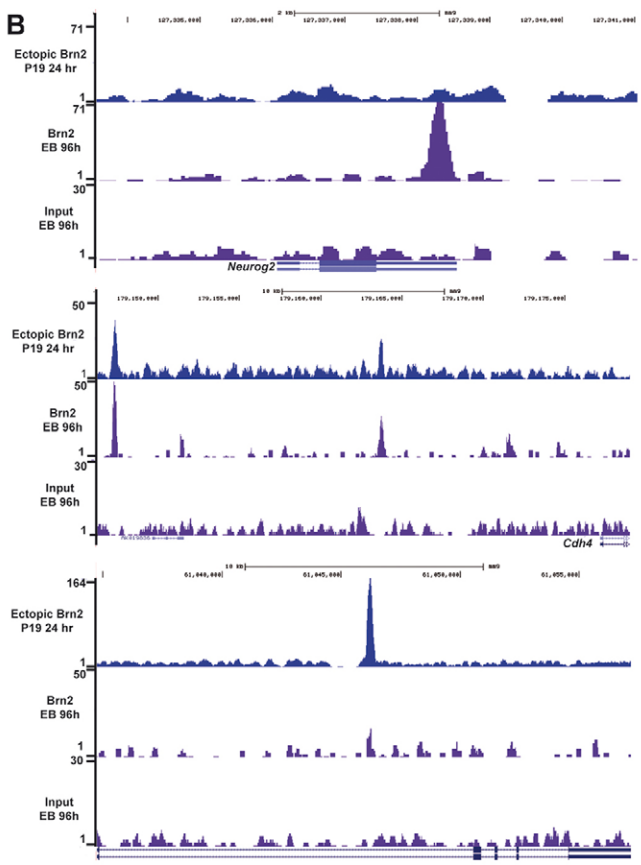

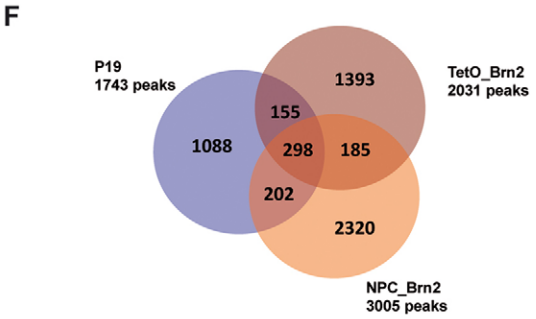

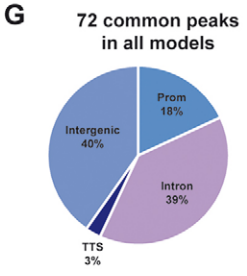

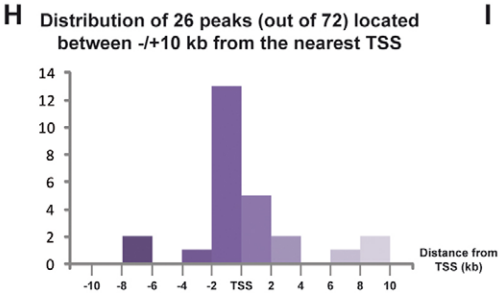

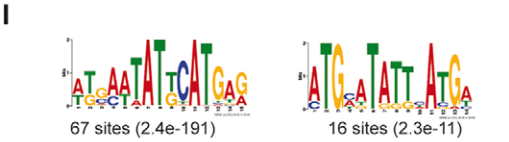

	MORE	MORE+1	Both
Highly conserved (72)	52 (72.2 %)	29 (40.3%)	11 (15.3%)

Fig. 5. Comparison of Brn2-occupied sites in retinoic-acid-treated embryoid bodies and P19 cells. (A) Venn diagrams indicating the overlap between the Brn2 sites in the indicated data sets. A MEME-ChIP analysis of the commonly occupied sites shows an enrichment in MORE-like motifs. (B) UCSC screenshot showing representative examples of common and specific peaks. (C) Table indicating the frequency of the indicated motifs at common and specific sites. (D) Ontology of the genes associated with the Brn2 sites commonly occupied in embryoid bodies and P19 cells. (E) Venn diagram indicating the overlap between genes associated with Brn2-occupied sites and downregulation following shBrn2 silencing in embryoid bodies and P19 cells. (F) Venn diagram indicating the overlap between genes associated with Brn2-occupied sites in P19 cells and NPCs with or without ectopic Brn2 expression. (G) Pie-chart showing distribution of the core set of 72 Brn2 sites in the genome. (H) A subset of core sites are enriched around the TSS. The graph shows a plot of the frequency of Brn2-occupied sites versus the distance to the TSS. (I) Core sites are highly enriched in MORE-like motifs.

Journal of Cell Science

Journal of Cell Science (2015) 128, 2303-2318 doi:10.1242/jcs.168849

To extend this analysis to three distinct models of neurogenesis, we integrated the data from retinoic-acid-induced embryoid bodies, Fgf2-induced NPCs and P19 cells. A total of 500 Brn2 sites were commonly occupied in Fgf2-induced NPCs and P19 cells and 453 were common between the P19 cells and the ESCs expressing ectopic Brn2 under the control of Tet0 (Fig. 5F). Of these sites, 298 were occupied under all three conditions. Comparing the 202 sites occupied in ESCs under all conditions with the 298 identified above identified 175 sites that were shared under all conditions in all models. This integrative analysis thus defines a set of Brn2-occupied sites and potentially regulated genes that form the core of the neurogenesis programme common to each model system.

Brn2, Ascl1 and Mytl1 cooperate to induce differentiation of fibroblasts into neurons (Vierbuchen et al., 2010). To investigate the mechanisms involved in this process, Wapinski et al. performed Brn2 ChIP-seq in fibroblasts in which these three factors had been ectopically expressed to induce differentiation (Wapinski et al., 2013). 2344 peaks were identified in fibroblasts and 5278 in the reprogrammed NPCs. Integrating this data identified 72 Brn2-occupied sites common to retinoic-acid-induced embryoid bodies, Fgf2-induced NPCs and P19 cells (Fig. 5G). These sites were enriched in promoters around the TSS (Fig. 5G,H), were highly enriched in MORE and MORE+1 motifs (Fig. 5I) and were associated with 91 potential target genes (supplementary material Table S4).

Zic1 is essential for neuronal differentiation of retinoic-acid-treated embryoid bodies

Amongst the 72 sites common to all current Brn2 ChIP-seq data sets, one prominent site lies 5′ to the *Zic1* and *Zic4* locus (see below). The Zic proteins have previously described roles in neural development (Ali et al., 2012; Merzdorf, 2007) and Zic1 expression is strongly downregulated in shBrn2-expressing retinoic-acid-induced embryoid bodies suggesting that it might be an important downstream effector of Brn2 function. Zic1 expression was silenced by lentivirus-mediated transfection of an shRNA against Zic1 (shZic1), resulting in impaired neuronal differentiation, with cell death and loss of the typical neuron-like morphology and strongly diminished axon formation of the surviving cells (Fig. 6A,B). Almost no Tubb3-expressing cells were observed after shZic1-mediated silencing and no axonal network could be observed (Fig. 6C). Moreover, only a few cells showed strong Pax6 labelling (supplementary material Fig. S1B). RNA-seq identified 101 downregulated genes strongly enriched in neurogenic functions (Fig. 6D). The 133 upregulated genes, by contrast, had diverse functions (Fig. 6E). A total of 49 of the 101 genes downregulated by shZic1 were also downregulated by shBrn2 (Fig. 6F). These genes are strongly enriched in neurogenic functions, but do not include Brn2 itself. Genes involved in neurogenesis such as *Epha8*, *Cdh8*, *Olig3* or *Zic3* were found among the 52 genes regulated uniquely by Zic1, showing that Zic1 activates a set of neurogenic genes complimentary to Brn2. By contrast, 33 of the 133 genes induced by shZic1 knockdown were also induced by shBrn2 knockdown, but are not associated with neurogenesis (Fig. 6G). These data are consistent with the idea that Brn2 binds to a site adjacent to *Zic1* to activate its expression. Consequently, Zic1 and Brn2 cooperate to regulate a set of downstream targets such as *Pax3*, *Pax7*, *Msx3*, *Zic4* or *Ncan* that are associated with Brn2-occupied sites and are down-regulated by silencing of *Brn2* and *Zic1*.

As mentioned above, amongst the 72 sites common to all current Brn2 ChIP-seq data sets, one prominent site lies 5′ to the *Zic1* and *Zic4* locus (Fig. 7A). This site comprises a MORE motif and a nearby ZFX-like motif as well as several E-boxes, through which Brn2 might cooperate with Ascl1 or other neurogenic bHLH factors to activate Zic1 expression (Fig. 7B). At present we know of no ChIP-grade antibodies for Zic1 and thus we are unable to determine which genes are associated with Zic1-occupied sites (but see note added in proof). As we detected a ZFX-like motif enriched at many Brn2-bound sites, we, however, tried to assess whether these sites could be recognised by Zic1, in agreement with possible cooperation between these factors.

To examine whether Brn2 could directly bind this site with or without Zic1, we performed electrophoresis mobility shift assay (EMSA) experiments with extracts from 293T cells transfected with vectors expressing Flag–Zic1 and/or HA–Brn2, or control un-transfected extracts, and oligonucleotides comprising the MORE and ZFX-like motifs from the Zic1 locus in a wild-type or mutated form. A specific retarded complex was seen only when HA–Brn2 was expressed using an oligonucleotide with the wild-type MORE showing that although Brn2 binds the MORE motif, there was no evidence for Zic1 binding (Fig. 7C). To confirm this, the retarded Brn2–MORE complex was first super-shifted and finally inhibited upon addition of increasing quantities of anti-HA antibody, whereas no effect was seen using anti-Flag antibody (Fig. 7D). These data show that Brn2 binds the MORE motif, but no evidence for binding of Zic1 to the ZFX motif was found.

We next tested whether this regulatory element could mediate transcription activation by Brn2 and/or Zic1. Two copies of the region encompassing the ZFX and MORE motifs (see bars in Fig. 7B) were cloned upstream of a chloramphenicol acetyltransferase (CAT) reporter construct with a minimal TATA-containing promoter (Kobi et al., 2010; Moutier et al., 2012) and transfected into 501Mel melanoma cells, where we have previously shown that Brn2 acts as an activator (Kobi et al., 2010). In the absence of ectopic Brn2 and Zic1 expression, the reporter vector with the *Zic1*-locus element had a low basal activity that was nevertheless increased compared to the corresponding empty vector, possibly owing to the action of the endogenous Brn2 in these cells (Fig. 7E). Ectopic expression of Brn2 or Zic1 activated CAT activity, whereas co-expression of the two proteins led to a much stronger activation. No effect was seen using the empty vector. Thus, despite the fact that we did not detect Zic1 binding by EMSA, this module acted as a functional Brn2- and Zic1-responsive element and mediated cooperative activation by these factors.

DISCUSSION

Brn2 is upstream of a neurogenic transcriptional network in retinoic-acid-treated embryoid bodies

We show that Brn2 expression is essential for the neurogenic fate of retinoic-acid-induced embryoid bodies. Retinoic-acid-treated embryoid bodies differentiate first into Pax6-expressing radial-glial-type NPCs. *In vivo*, radial glial cells are essential for the development of most cortical neurons (Götz and Barde, 2005; Malatesta et al., 2003). Given the important role of Brn2 (and Zic1) in the developing cortex, it is not surprising that Brn2 plays a crucial role in the differentiation of retinoic-acid-treated embryoid bodies *in vitro*. However, two features distinguish the *in vitro* and *in vivo* scenarios. Firstly, *in vivo* Brn1 and Brn2 play redundant roles in the cortex and a clear phenotype is observed only upon double knockout (Sugitani et al., 2002). In contrast, Brn2 plays a predominant role *in vitro* in embryoid bodies cells, despite expression of the closely related Brn1 (Pou3f3), whose mRNA is

Journal of Cell Science (2015) 128, 2303-2318 doi:10.1242/jcs.168849

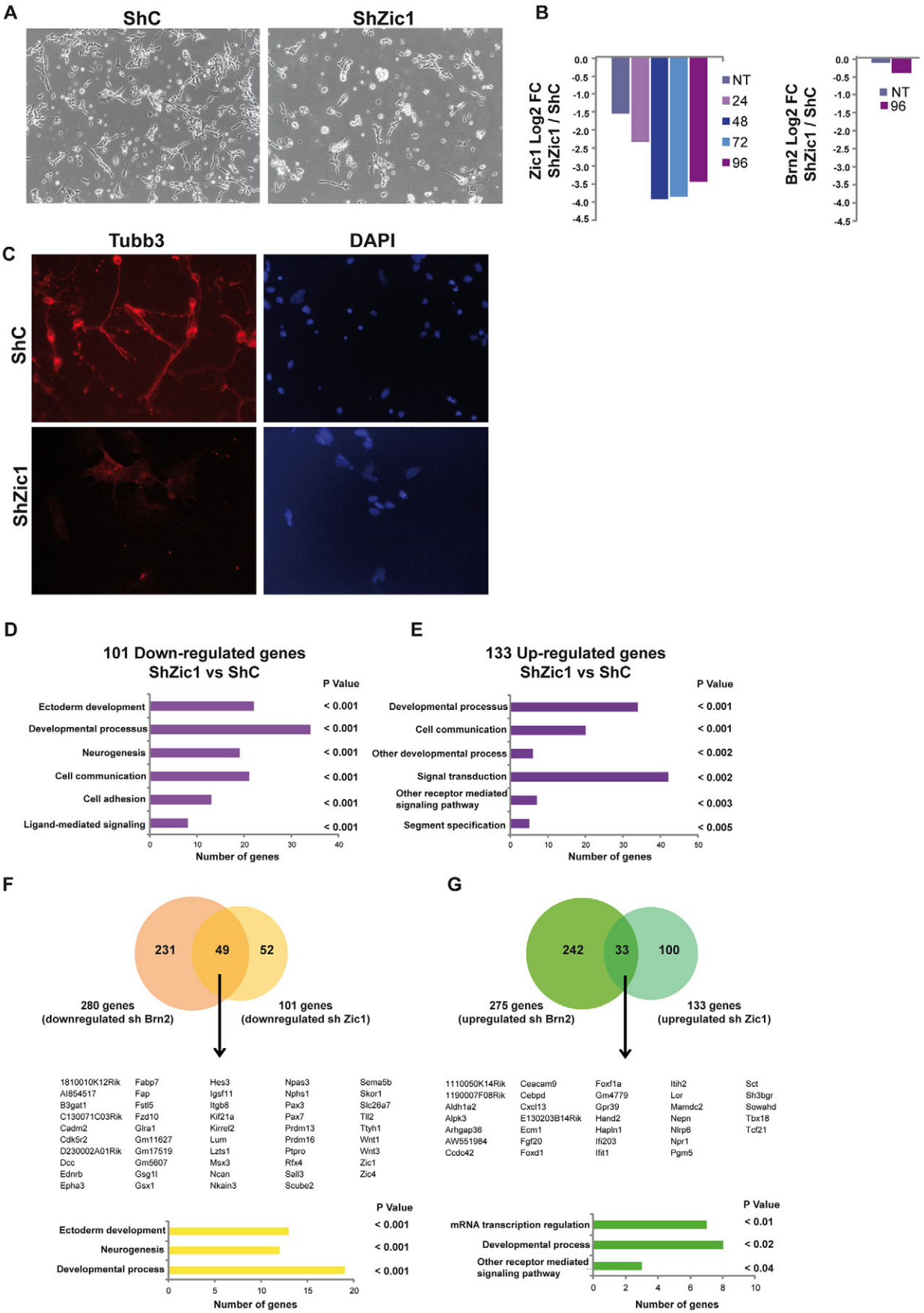

Fig. 6. See next page for legend.

Journal of Cell Science

Journal of Cell Science (2015) 128, 2303-2318 doi:10.1242/jcs.168849

Fig. 6. Zic1 is essential for neuronal differentiation of embryoid bodies. (A) Phase contrast microscopy images of cells expressing the indicated shRNAs 24 h after dissociation of the embryoid bodies. Images were taken at 20× magnification. (B) *Zic1* and *Brn2* expression in ShC and ShZic1 cells as measured by RT-qPCR. Results show the mean of three experiments. FC, fold change; NT, not treated. (C) Immunofluoresence performed on shC and shZic1 cells with antibody against Tubb3 and counterstained with DAPI. Note that these cells represent an experiment independent from B. (D,E) Ontology analysis of genes whose expression was up- or down-regulated following Zic1 knockdown. (F,G) Venn diagrams illustrating overlap between genes up- and down-regulated upon Brn2 and Zic1 silencing along with ontology analysis.

strongly upregulated in retinoic-acid-treated embryoid bodies and not significantly affected by Brn2 silencing. Brn1 expression cannot, therefore, compensate for Brn2 loss in ESCs in contrast to their partially redundant roles *in vivo*. Secondly, although Brn2 is expressed in ESC-derived radial glial cells *in vitro*, it is not expressed in radial glial cells of the ventricular zone in the developing cortex, but rather at later stages of differentiation in the sub-ventricular zone (Hagino-Yamagishi et al., 1997).

Despite these differences, Brn2 controls a large set of neurogenic genes in retinoic-acid-treated embryoid bodies. Brn2 binds the *Ascl1* and *Neurog1* loci and their expression is strongly downregulated by Brn2 silencing. Ascl1 and Neurog1 are crucial transcription factors in neurogenesis and loss of their expression strongly contributes to the loss of neural fate. Nevertheless, *Ascl1* expression initiates somewhat before that of *Brn2*, suggesting that Brn2 is not essential for its initial activation, but to maintain its expression at later stages.

Brn2 also regulates Notch signalling because expression of *Dll1*, *Dll3*, *Jag1*, *Hes3* and *Hes5* was strongly downregulated. Ascl1 and Brn2 cooperate to activate *Dll1 in vivo* in the chick neural tube and in P19 cells (Castro et al., 2006). This cooperativity is dependent on a promoter element comprising an OCT motif flanked by two E-box binding sites for Ascl1 (Castro et al., 2006). A similar element is found in the promoter of *Dll3* and other effectors of Notch signalling as well as other neurogenic genes (Castro et al., 2006). Nevertheless, in retinoic-acid-induced embryoid bodies and P19 cells, we did not observe Brn2 occupancy of the OCT motifs in the *Dll1* and *Dll3* promoters by ChIP-seq, although it could be argued that this could occur at a later stage in P19 cells. In retinoic-acid-induced embryoid bodies, activation of these genes is dependent on Brn2, but this is an indirect effect probably that is probably mediated by Ascl1 and/or Neurog1, direct targets of Brn2. Hence, in contrast to the cooperative model for activation of these target genes *in vivo* (Castro et al., 2006), in retinoic-acid-induced embryoid bodies their activation is a hierarchical process where Brn2 activates Ascl1 and Neurog1, which in turn activate target gene expression.

Note also that the OCT motif is not a preferred site for Brn2, which preferentially binds MORE elements. The elements described above do not have the full MORE consensus sequence. It is therefore possible that another POU factor occupies these sites and cooperates with Ascl1 in retinoic-acid-induced embryoid bodies. Furthermore, we did not detect E-box-binding factors amongst those that were enriched at Brn2-occupied MORE and MORE+1 sites, although they were present at some crucial sites such as the *Zic1* locus.

Definition of a potential core neurogenic Brn2-regulated regulatory network identifies a Brn2–Zic1 axis

As with most transcription factors, only some of Brn2-occupied sites are likely to be functional. To define sites and target genes crucial for Brn2 function, we integrated our ChIP-seq data with other public data sets. We were surprised to find that Brn2 genome occupancy was very different in Fgf2- and retinoic-acid-induced NPCs and further integration of data from P19 cells and reprogrammed fibroblasts identified only 72 common sites.

Some of the differences in Brn2 genomic occupancy in the different models might be accounted for by dynamic genome occupancy that can evolve as differentiation proceeds, reflecting the fact that no two data sets were made at exactly the same stage in the differentiation process. Alternatively, they might reflect inherent differences in the pathways that induce neurogenesis in the different models where the initial stimuli are the resulting neuronal populations differ. Irrespective of the underlying causes, our analysis pinpointed a common set of sites and associated target genes that might form the core of the Brn2-induced neurogenic programme.

Among the 91 Brn2 common target genes is the atypical cadherin Fat4, which is regulated by Brn2 in retinoic-acid-treated embryoid bodies. Fat4 is involved in planar cell polarity signalling, and mutations in human FAT4 and its receptor DCHS1 are associated with Van Maldergem syndrome, which is characterised by abnormal positioning of neurons in the cerebral cortex of patients (Cappello et al., 2013). Knockdown of these proteins in the mouse show they are important in neuroprogenitor cell proliferation, maintenance of the progenitor state and positioning of cells within the proliferative zones of the developing brain. Similarly, Fat4 is also important for facial migration of branchiomotor neurons (Zakaria et al., 2014) and for cranial neural tube formation (Saburi et al., 2012). All of these data point to an important role of Fat4 in the differentiation and migration of cortical neurons, hallmarks of Brn2 function during brain development in mouse. Fat4 might therefore be a crucial downstream target gene of Brn2 in embryoid bodies and *in vivo* in cortex development. Among the other common Brn2 targets is Pou6f1 (also known as Brn5), which is expressed in myelinating Schwann cells whose development is regulated by Brn2 (Jaegle et al., 2003). Pou6f1 might therefore be a direct downstream target of Brn2 in these cells.

We further identified a common and prominent Brn2 site located in the locus encoding Zic1 and Zic4. Zic1 and Zic4 have been associated with Dandy–Walker syndrome and cerebellum development (Merzdorf, 2007; Inoue et al., 2007; Grinberg et al., 2004). In retinoic-acid-treated embryoid bodies, Zic1 silencing diminished neuronal differentiation without loss of Brn2 expression. Brn2 is thus essential, but not sufficient to specify neuronal fate and cooperates with its downstream target Zic1. Interestingly, the Brn2-binding site defines a regulatory module acting as a Brn2- and Zic1-responsive element, mediating cooperative activation by these factors. These findings show that Brn2 and Zic1 can actually cooperate to activate gene expression through a natural response element. We noted that during differentiation, Zic1 expression initiates before that of Brn2, yet Brn2 is subsequently required to maintain Zic1 expression. The finding that these factors cooperatively activate expression through this element likely accounts for the diminished Zic1 expression upon Brn2 silencing. Among the other target genes that are regulated by Brn2 and Zic1 are *Wnt1* and *Wnt3*, which is consistent with the known role of Zic1 in regulating Wnt expression in neurectoderm patterning and development of the neural crest (Merzdorf, 2007; Merzdorf and Sive, 2006).

In conclusion, our results reveal the crucial role of a Brn2–Zic1 axis is specifying the neuronal fate of retinoic-acid-treated ESCs. Brn2 activates Zic1 expression and, both individually and together, these factors regulate expression of the downstream neurogenic

Journal of Cell Science (2015) 128, 2303-2318 doi:10.1242/jcs.168849

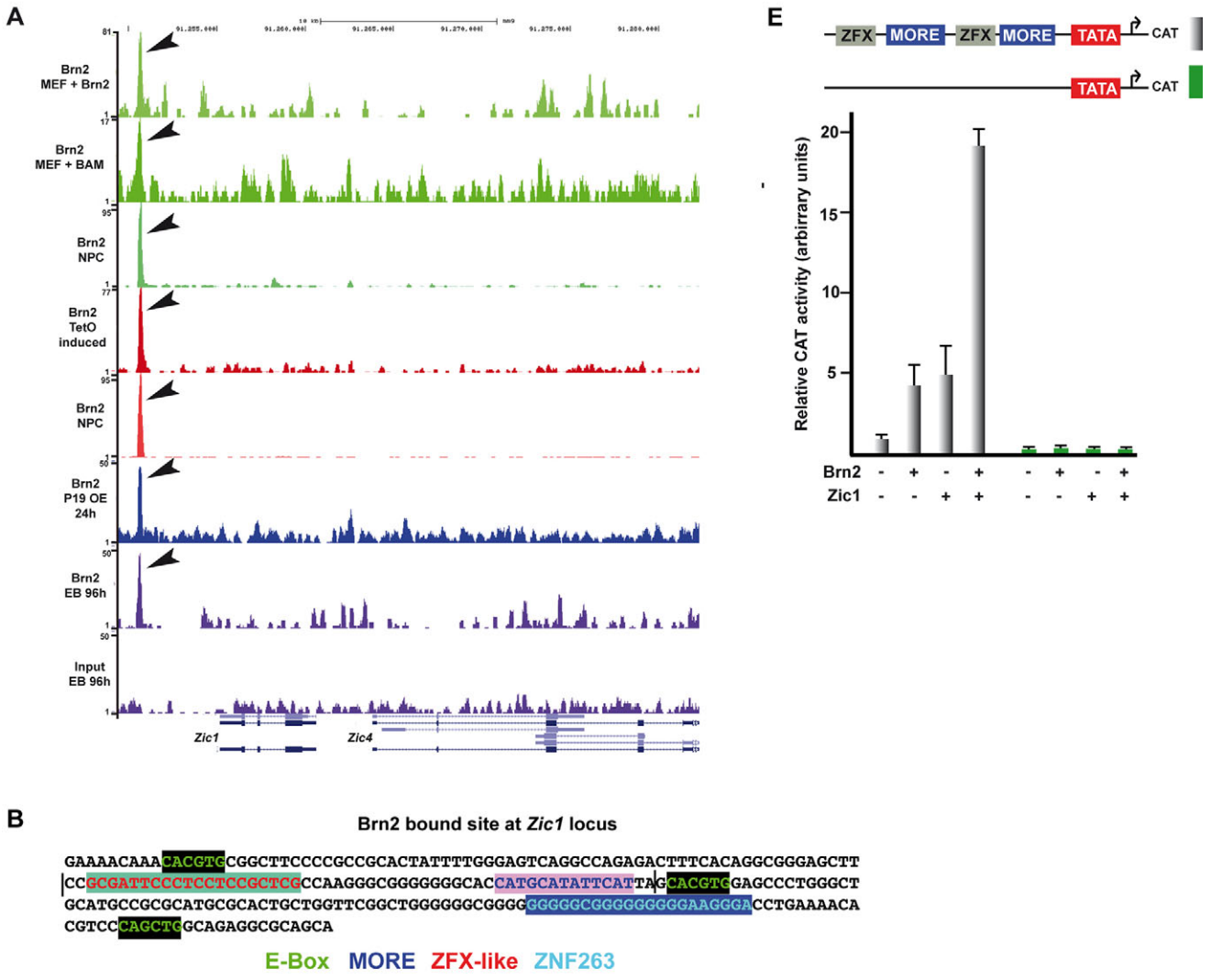

Fig. 7. See next page for legend.

Journal of Cell Science (2015) 128, 2303-2318 doi:10.1242/jcs.168849

Fig. 7. Identification of Brn2- and Zic1-responsive element at a common core Brn2-occupied site. (A) UCSC screenshots illustrating a conserved Brn2-binding site in the *Zic1*, *Zic4* locus. (B) The DNA sequence around the MORE motif bound by Brn2 at the *Zic1* locus is shown and the presence of several other sequence motifs is indicated by coloured boxes. (C) EMSA using double-stranded 67-bp oligonucleotides centred on the MORE motif and comprising the additional motifs boxed in A in either wild-type or mutated form, as indicated. Extracts are from 293T cells transfected with vectors expressing HA-tagged Brn2 and/or Flag (F)-tagged Zic1 as shown above each lane. NE indicates probe alone with no extract. (D) EMSA performed with WT oligonucleotide and the indicated transfected cells extracts with increasing quantities of either Flag or HA antibody. The asterisk shows the super-shifted Brn2–MORE complex. (E) CAT reporter assays. The CAT reporter vectors are schematised above the graph. The CAT activity of each reporter in the absence or presence of ectopically expressed Brn2 and/or Zic1 is indicated. Results are mean±s.d. (n=3).

programme. As the Brn2 site in the Zic1 locus is present in all the models analysed here, this axis might be more of more general relevance to neurogenic differentiation and reprogramming.

MATERIALS AND METHODS

Cell culture and generation of stable cell lines

Lentiviral cell lines were generated using shRNA vectors obtained from Sigma (Mission sh-RNA series) in the PLKO vector. Viral supernatants were obtained by transfection of HEK293T cell lines with the PLKO-shBrn2 (shBrn2 sequence, 5′-AGGCGGATCAAACTCGGATTT-3′) or PLKO-shZic1 (shZic1 sequence, 5′-CCAGCGCTGCTTTCAATTCTA-3′). Co-transfection with PLP1, PLP2 and PLP-VSVG vectors (Sigma) was used to produce viral particles. Supernatants of co-transfected HEK293T cells were collected 48 h after transfection and used to infect ESCs or P19 cells. Stable ESCs and P19 cells were selected 2 days after infection with puromycin (1 µg/ml). Western blotting was performed with anti-Brn2 antibody (Santa Cruz Biotechnology, SC-6029).

For generation of ESC or P19 lines overexpressing Brn2, cells were co-transfected with a vector containing 3HA–Brn2 under the control of an retinoic-acid-inducible promoter (5×DR5) and a second vector encoding puromycin resistance. Transfected cells were selected with 1 µg of puromycin and overexpression of tagged protein was verified by western blotting using the 12CA5 anti-HA antibody (Roche, Basel, Switzerland).

Neuronal differentiation of ESCs and P19 cells

ES J1 cell differentiation was performed as previously described (Bibel et al., 2007, 2004). Briefly, ESCs were grown and amplified on feeder cells in Dulbecco's modified Eagle's medium (DMEM, 4.5 g/l glucose) with GLUTAMAX-I containing 15% fetal calf serum (FCS) and leukemia inhibitory factor (LIF). After feeder cell depletion, 4×10^6 ESCs were plated on non-adherent bacterial dishes in medium containing 10% serum to form embryoid bodies that were treated with 5×10^{-6} M of all-trans retinoic acid for 4 days. Samples were collected at several time points to perform further RNA or protein extraction. Neuronal differentiation was completed by dissociation of embryoid bodies using Trypsin-EDTA 0.05% (Invitrogen) and 2.5×10^6 cells were plated on a 25-mm^2 plate coated with poly-DL-ornithine and laminin. After 1 day in DMEM with Ham's F12 medium complemented with BSA and N2-supplement, early differentiated neurons were obtained.

P19 cells were differentiated into neurons using a protocol adapted from previously described experiments (Gao et al., 2001). Briefly, P19 cells were amplified in DMEM (1 g/l glucose) with 10% FCS. To perform neuronal differentiation, 3×10^6 M cells were plated in P10 bacterial dishes (Greiner) in presence of 5×10^{-6} M retinoic acid. After 4 days, aggregates were dissociated in trypsin (2.5%) and 2.5×10^6 cells were plated on a 60-mm^2 plate coated with poly-L-lysine.

Immunofluorescence

After 96 h of retinoic acid treatment, the embryoid bodies were dissociated and cultured on glass slides for 24 h under conditions for neuronal progenitor differentiation. Cells were fixed in 4% paraformaldehyde, then blocked and permeabilized with phosphate-buffered saline (PBS) containing 2% BSA and 0.2% Triton X-100. After incubation with primary antibodies against Brn2 (1:500; sc-6029X, Santa Cruz Biotechnology, Santa Cruz, CA), Tubb3 (1:500; MMS-435P Covence, Dedham, MA) and PAX6 (1:100; PRB-278P Covence, Dedham MA), for 24 h at 4°C followed by three washes in PBS, cells were incubated with the Alexa-Fluor-594-conjugated secondary antibodies or with Cy3-conjugated secondary antibodies diluted at 1:100 in PBS containing BSA and Triton X-100 for 1 h at room temperature. Nuclei were stained with 4,6-diamidino-2-phenylindole (DAPI) diluted at 1:1000 in PBS. The cells were then mounted in antifading medium (Vectashield, Vector laboratories, Inc. Birlingame, CA) and observed with an epifluorescence microscope (Carl Zeiss, Göttingen, Germany).

mRNA preparation, quantitative PCR and RNA-seq

RNA isolation was performed according to standard procedure using the kit from Sigma. RT-qPCR was carried out with SYBR® Green I (Qiagen) and Multiscribe reverse transcriptase (Invitrogen) and monitored using a LightCycler® 480 (Roche). Primer sequences for cDNA were designed using Primer3Plus software. *Gapdh* expression was used as to normalise the results.

For RNA-sequencing, mRNA was isolated from two independent experiments. mRNA-seq was performed essentially as described previously (Herquel et al., 2013) with libraries of template molecules suitable for high-throughput DNA sequencing created using a TruSeq™ RNA Sample Preparation v2 kit (Illumina). Reads were mapped onto the mm9 assembly of the *Mus musculus* genome by using Tophat version 1.4.1 (Trapnell et al., 2009; Trapnell and Salzberg, 2009) and Bowtie version 0.12.7 (Langmead et al., 2009). Quantification of gene expression was performed using HTSeq-0.5.3p5. Comparisons were performed using the statistical method proposed previously (Anders and Huber, 2010). Resulting P-values were adjusted for multiple testing by using the method of Benjamini and Hochberg (Benjamini and Hechtlinger, 2014; Benjamini and Yekutieli, 2005). Significantly deregulated genes were selected using a $\log_2$ fold change of >1 or <−1 and an adjusted P-value cutoff of 0.1. Gene ontology analysis were performed using the functional annotation clustering function of DAVID (http://david.abcc.ncifcrf.gov/home.jsp).

ChIP-seq analysis

ChIP-seq experiments were performed on chromatin from embryoid bodies or P19 aggregates dissociated by douncing directly in crosslinking solution (0.4% PFA). Sonication and ChIP were performed as previously described (Herquel et al., 2013). The ChIP-grade anti-Brn2 antibody (Sc 6029-X) and anti-H3K27ac antibody (number 39133; Active Motif) were used.

ChIP-seq libraries were prepared and sequenced as previously described (Choukrallah et al., 2012; Herquel et al., 2013). Peak detection was performed using the MACS software (http://liulab.dfci.harvard.edu/MACS/) (Zhang et al., 2008) using the corresponding input as control with default settings. *De novo* motif search was done using MEME-ChIP software (http://meme.nbcr.net/meme/cgi-bin/meme-chip.cgi). ChIP-seq peak annotation was performed using Homer, individual motif occurrences were detected by FIMO; both pieces of software are available on IGBMC Galaxy platform (www.galaxeast.fr). Co-occurrence analysis was performed as follows. The analysis was initiated by detecting known motifs using FIMO within regions of interest given as input. From FIMO results, two PERL scripts computed the frequency of occurrence of each motif and of co-occurring motifs. Two motifs were considered as co-occurring if they were present in the same sequence. This analysis was performed once on the input BED file and n times on randomly selected regions. Region size distribution of the randomly selected regions was the same as for the input BED file. Randomly selected regions were used to compute an expected distribution of motif occurrence or motif co-occurrence. The significance of the motif occurrence and co-occurrence was estimated through the computation of a Z-score computed as: $z=(x-\mu)/\sigma$, where x is the observed value (number of motif occurrence or co-occurrence), μ is the mean of the number of occurrences or co-occurrences of motifs (computed over controls) and σ is the standard deviation of the number of occurrences or co-occurrences of motifs (computed over controls). Z-scores were subsequently turned into P-values and a multi-testing correction was applied (Benjamini and Hechtlinger, 2014; Benjamini and Yekutieli, 2005). Common peaks in the different data

sets were called using the 'Intersect' function of Galaxeast, which detects peaks with at least one overlapping nucleotide within a window of 200 nucleotides centred on the peak summit.

EMSAs

EMSA assays were performed as previously described (Moutier et al., 2012). Oligonucleotides used were as follows: wild-type sense and antisense, 5′-GAGCTTCCGCGATTCCCTCCTCCGCTCGCCAAGGGCGGGGGGGCACCATGCATATTCATTAGCACGTACGTGCTAATGAATATGCATGGTGCCCCCCCGCCCTTGGCGAGCGGAGGAGGGAATCGCGGAAGCTC-3′; MORE mutant sense and antisense, 5′-GAGCTTCCGCGATTCCCTCCTCCGCTCGCCAAGGGCGGGGGGGCACCATGCA**CCG**TCATTAGCACGTACGTGCTAATGACGGTGCATGGTGCCCCCCCGCCCTTGGCGAGCGGAGGAGGGAATCGCGGAAGCTC-3′; MORE and ZFX mutant sense and antisense, 5′-GAGCTTCC**AT**GATT**A**C**A**TCCT**ATTA**TCGCCAAGGGCGGGGGGGCACCATGCA**CCG**TCATTAGCACGTACGTGCTAATGACGGTGCATGGTGCCCCCCCGCCCTTGGCGATAATAGGATGTAATCATGGAAGCTC-3′. Bold nucleotides indicate the position of the mutations.

Chloramphenicol acetyl transferase reporter assays

For reporter assays, 501Mel cells were transfected with 1 µg of the TATA-chloramphenicol acetyl transferase (CAT) reporter comprising two copies of the Zic1 locus regulatory element or empty vector, 1 µg pCH110 expressing β-galactosidase as internal standard, and 1 µg of pCMV HA–Brn2 and/or Flag–Zic1 expression vectors. Transfections were performed in triplicate with Fugene (Roche, Basel Switzerland). Extract preparation, β-galactosidase assays and CAT assays were performed using a Roche CAT-Elisa kit as previously described (Mengus et al., 2005). To generate the TATA-CAT reporter plasmids, oligonucleotides comprising the sequence initiating at 5′-CCGCGAT upstream of the ZFX motif and terminating at TTCATTA-3′ immediately after the MORE motif (see Fig. 7B) were cloned with asymmetric BglII-EcoR1-Nde1 restriction sites upstream of the TATA element.

Note added in proof

While this manuscript was being revised, Frank et al. published ChIP-seq data for Zic1 and Zic2 in post-natal day-7 mouse cerebellum (Frank et al., 2015). Given the functional relationship between Brn2 and Zic1 described in this paper, we integrated this new public ChIP-seq data with the Brn2 data in our paper. First, we observed that Zic1 binding is seen in day-7 mouse cerebellum at the common Brn2 binding site characterised in this paper upstream of the *Zic1-Zic4* locus, confirming our conclusion that this site integrates Brn2 and Zic1 signalling. Second, Zic1 and Zic2 show a prominent and complex pattern of multiple binding sites throughout the *Zic1-Zic4* locus perhaps indicative of auto-regulation. Third, a global analysis identified a large overlap between Brn2-binding sites in embryoid bodies treated with retinoic acid for 96 h and Zic1 and Zic2 binding in day-7 cerebellum, with Zic1-Brn2 co-localisation at 887 sites. While this represents 20% of the Zic1-occupied sites, it represents 42% of the Brn2-occupied sites. Fourth, Zic1 and Zic2 also show multiple prominent binding sites over the *Pou3f2* gene locus, encoding Brn2, showing the potential for reciprocal Zic1–Brn2 transcriptional regulation.

Taken together, these results further lend weight to the idea that a Brn2-Zic1 axis might play an important role not only in differentiating ESCs, but also *in vivo* in mouse cerebellum.

Acknowledgements

We thank, I. Michel for excellent technical assistance and CAT assays, Y. Barde for the gift of J1 ESCs, C. Keime and A. Velt for RNA-seq analysis, B. Jost, and all the staff of the IGBMC high-throughput sequencing facility, a member of 'France Génomique' consortium (ANR10-INBS-09-08), Y. Davidson for help with data analysis, and M. Hestin and G. Rossi for assistance with ESC culture.

Competing interests

The authors declare no competing or financial interests.

Author contributions

S.U. performed and analysed experiments on retinoic acid-treated embryoid bodies and analysed the data from the P19 cells and public data sets together with D.K. and S.LG. D.K. performed the experiments on the P19 cells and performed bioinformatics analysis. D.L. performed initial shZic1 silencing. M.E. performed the knockdowns and immunostaining. S.L.G. and T.Y. assisted in bioinformatics analysis of the motif co-occurrence and peak detection respectively. I.D. S.U. and D.K. conceived experiments, analysed data, I.D. and S.U. wrote the paper.

Funding

This work was supported by grants from the Centre national de la recherche scientifique (CNRS); the Institut national de la santé et de la recherche médicale (INSERM); the Ligue Nationale et Départementale Région Alsace contre le Cancer; the Institut National du Cancer (INCa); and the Agence national de la recherche [grant number ANR-10-LABX-0030-INRT]. All were under the frame programme Investissements d'Avenir [grant numbers ANR-10-IDEX-0002-02 and project grant ANR-11-BSV8-023]. I.D. is an 'équipe labellisée' of the Ligue Nationale contre le Cancer.

Supplementary material

Supplementary material available online at
http://jcs.biologists.org/lookup/suppl/doi:10.1242/jcs.168849/-/DC1

References

Agoston, Z., Heine, P., Brill, M. S., Grebbin, B. M., Hau, A.-C., Kallenborn-Gerhardt, W., Schramm, J., Gotz, M. and Schulte, D. (2014). Meis2 is a Pax6 co-factor in neurogenesis and dopaminergic periglomerular fate specification in the adult olfactory bulb. *Development* **141**, 28-38.

Al Tanoury, Z., Gaouar, S., Piskunov, A., Ye, T., Urban, S., Jost, B., Keime, C., Davidson, I., Dierich, A. and Rochette-Egly, C. (2014). Phosphorylation of the retinoic acid receptor RARgamma2 is crucial for the neuronal differentiation of mouse embryonic stem cells. *J. Cell Sci.* **127**, 2095-2105.

Alazard, R., Blaud, M., Elbaz, S., Vossen, C., Icre, G., Joseph, G., Nieto, L. and Erard, M. (2005). Identification of the 'NORE' (N-Oct-3 responsive element), a novel structural motif and composite element. *Nucleic Acids Res.* **33**, 1513-1523.

Ali, R. G., Bellchambers, H. M. and Arkell, R. M. (2012). Zinc fingers of the cerebellum (Zic): transcription factors and co-factors. *Int. J. Biochem. Cell Biol.* **44**, 2065-2068.

Anders, S. and Huber, W. (2010). Differential expression analysis for sequence count data. *Genome Biol.* **11**, R106.

Ballas, N. and Mandel, G. (2005). The many faces of REST oversee epigenetic programming of neuronal genes. *Curr. Opin. Neurobiol.* **15**, 500-506.

Benjamini, Y. and Hechtlinger, Y. (2014). Discussion: an estimate of the science-wise false discovery rate and applications to top medical journals by Jager and Leek. *Biostatistics* **15**, 13-16; discussion 39-45.

Benjamini, Y. and Yekutieli, D. (2005). Quantitative trait Loci analysis using the false discovery rate. *Genetics* **171**, 783-790.

Bibel, M., Richter, J., Schrenk, K., Tucker, K. L., Staiger, V., Korte, M., Goetz, M. and Barde, Y.-A. (2004). Differentiation of mouse embryonic stem cells into a defined neuronal lineage. *Nat. Neurosci.* **7**, 1003-1009.

Bibel, M., Richter, J., Lacroix, E. and Barde, Y.-A. (2007). Generation of a defined and uniform population of CNS progenitors and neurons from mouse embryonic stem cells. *Nat. Protoc.* **2**, 1034-1043.

Botquin, V., Hess, H., Fuhrmann, G., Anastassiadis, C., Gross, M. K., Vriend, G. and Scholer, H. R. (1998). New POU dimer configuration mediates antagonistic control of an osteopontin preimplantation enhancer by Oct-4 and Sox-2. *Genes Dev.* **12**, 2073-2090.

Cao, X., Pfaff, S. L. and Gage, F. H. (2008). YAP regulates neural progenitor cell number via the TEA domain transcription factor. *Genes Dev.* **22**, 3320-3334.

Cappello, S., Gray, M. J., Badouel, C., Lange, S., Einsiedler, M., Srour, M., Chitayat, D., Hamdan, F. F., Jenkins, Z. A., Morgan, T. et al. (2013). Mutations in genes encoding the cadherin receptor-ligand pair DCHS1 and FAT4 disrupt cerebral cortical development. *Nat. Genet.* **45**, 1300-1308.

Castro, D. S. and Guillemot, F. (2011). Old and new functions of proneural factors revealed by the genome-wide characterization of their transcriptional targets. *Cell Cycle* **10**, 4026-4031.

Castro, D. S., Skowronska-Krawczyk, D., Armant, O., Donaldson, I. J., Parras, C., Hunt, C., Critchley, J. A., Nguyen, L., Gossler, A., Göttgens, B. et al. (2006). Proneural bHLH and Brn proteins coregulate a neurogenic program through cooperative binding to a conserved DNA motif. *Dev. Cell* **11**, 831-844.

Choukrallah, M.-A., Kobi, D., Martianov, I., Pijnappel, W. W. M. P., Mischerikow, N., Ye, T., Heck, A. J. R., Timmers, H. T. M. and Davidson, I. (2012). Interconversion between active and inactive TATA-binding protein transcription complexes in the mouse genome. *Nucleic Acids Res.* **40**, 1446-1459.

Cook, A. L. and Sturm, R. A. (2008). POU domain transcription factors: BRN2 as a regulator of melanocytic growth and tumourigenesis. *Pigment Cell Melanoma Res.* **21**, 611-626.

Frank, C. L., Liu, F., Wijayatunge, R., Song, L., Biegler, M. T., Yang, M. G., Vockley, C. M, Safi, A., Gersbach, C. A., Crawford, G. E. et al. (2015). Regulation of chromatin accessibility and Zic binding at enhancers in the developing cerebellum. *Nat. Neurosci.* **18**, 647-656.

Fujii, H. and Hamada, H. (1993). A CNS-specific POU transcription factor, Brn-2, is required for establishing mammalian neural cell lineages. *Neuron* **11**, 1197-1206.

Gao, X., Bian, W., Yang, J., Tang, K., Kitani, H., Atsumi, T. and Jing, N. (2001). A role of N-cadherin in neuronal differentiation of embryonic carcinoma P19 cells. *Biochem. Biophys. Res. Commun.* **284**, 1098-1103.

Götz, M. and Barde, Y.-A. (2005). Radial glial cells defined and major intermediates between embryonic stem cells and CNS neurons. *Neuron* **46**, 369-372.

Grinberg, I., Northrup, H., Ardinger, H., Prasad, C., Dobyns, W. B. and Millen, K. J. (2004). Heterozygous deletion of the linked genes ZIC1 and ZIC4 is involved in Dandy-Walker malformation. *Nat. Genet.* **36**, 1053-1055.

Hagino-Yamagishi, K., Saijoh, Y., Ikeda, M., Ichikawa, M., Minamikawa-Tachino, R. and Hamada, H. (1997). Predominant expression of Brn-2 in the postmitotic neurons of the developing mouse neocortex. *Brain Res.* **752**, 261-268.

Herquel, B., Ouararhni, K., Martianov, I., Le Gras, S., Ye, T., Keime, C., Lerouge, T., Jost, B., Cammas, F., Losson, R. et al. (2013). Trim24-repressed VL30 retrotransposons regulate gene expression by producing noncoding RNA. *Nat. Struct. Mol. Biol.* **20**, 339-346.

Hogan, B. L. (1996). Bone morphogenetic proteins: multifunctional regulators of vertebrate development. *Genes Dev.* **10**, 1580-1594.

Inoue, T., Ota, M., Ogawa, M., Mikoshiba, K. and Aruga, J. (2007). Zic1 and Zic3 regulate medial forebrain development through expansion of neuronal progenitors. *J. Neurosci.* **27**, 5461-5473.

Jaegle, M., Ghazvini, M., Mandemakers, W., Piirsoo, M., Driegen, S., Levavasseur, F., Raghoenath, S., Grosveld, F. and Meijer, D. (2003). The POU proteins Brn-2 and Oct-6 share important functions in Schwann cell development. *Genes Dev.* **17**, 1380-1391.

Klemm, J. D. and Pabo, C. O. (1996). Oct-1 POU domain-DNA interactions: cooperative binding of isolated subdomains and effects of covalent linkage. *Genes Dev.* **10**, 27-36.

Klemm, J. D., Rould, M. A., Aurora, R., Herr, W. and Pabo, C. O. (1994). Crystal structure of the Oct-1 POU domain bound to an octamer site: DNA recognition with tethered DNA-binding modules. *Cell* **77**, 21-32.

Kobi, D., Steunou, A.-L., Dembélé, D., Legras, S., Larue, L., Nieto, L. and Davidson, I. (2010). Genome-wide analysis of POU3F2/BRN2 promoter occupancy in human melanoma cells reveals Kitl as a novel regulated target gene. *Pigment Cell Melanoma Res.* **23**, 404-418.

Koga, M., Matsuda, M., Kawamura, T., Sogo, T., Shigeno, A., Nishida, E. and Ebisuya, M. (2014). Foxd1 is a mediator and indicator of the cell reprogramming process. *Nat. Commun.* **5**, 3197.

Langmead, B., Trapnell, C., Pop, M. and Salzberg, S. L. (2009). Ultrafast and memory-efficient alignment of short DNA sequences to the human genome. *Genome Biol.* **10**, R25.

Lodato, M. A., Ng, C. W., Wamstad, J. A., Cheng, A. W., Thai, K. K., Fraenkel, E., Jaenisch, R. and Boyer, L. A. (2013). SOX2 co-occupies distal enhancer elements with distinct POU factors in ESCs and NPCs to specify cell state. *PLoS Genet.* **9**, e1003288.

Mahony, S., Mazzoni, E. O., McCuine, S., Young, R. A., Wichterle, H. and Gifford, D. K. (2011). Ligand-dependent dynamics of retinoic acid receptor binding during early neurogenesis. *Genome Biol.* **12**, R2.

Malatesta, P., Hack, M. A., Hartfuss, E., Kettenmann, H., Klinkert, W., Kirchhoff, F. and Götz, M. (2003). Neuronal or glial progeny: regional differences in radial glia fate. *Neuron* **37**, 751-764.

Mark, M., Ghyselinck, N. B. and Chambon, P. (2006). Function of retinoid nuclear receptors: lessons from genetic and pharmacological dissections of the retinoic acid signaling pathway during mouse embryogenesis. *Annu. Rev. Pharmacol. Toxicol.* **46**, 451-480.

McEvilly, R. J., de Diaz, M. O., Schonemann, M. D., Hooshmand, F. and Rosenfeld, M. G. (2002). Transcriptional regulation of cortical neuron migration by POU domain factors. *Science* **295**, 1528-1532.

Mengus, G., Fadloun, A., Kobi, D., Thibault, C., Perletti, L., Michel, I. and Davidson, I. (2005). TAF4 inactivation in embryonic fibroblasts activates TGFbeta signalling and autocrine growth. *EMBO J.* **24**, 2753-2767.

Merzdorf, C. S. (2007). Emerging roles for zic genes in early development. *Dev. Dyn.* **236**, 922-940.

Merzdorf, C. S. and Sive, H. L. (2006). The zic1 gene is an activator of Wnt signaling. *Int. J. Dev. Biol.* **50**, 611-617.

Millevoi, S., Thion, L., Joseph, G., Vossen, C., Ghisolfi-Nieto, L. and Erard, M. (2001). Atypical binding of the neuronal POU protein N-Oct3 to noncanonical DNA targets. Implications for heterodimerization with HNF-3 beta. *Eur. J. Biochem.* **268**, 781-791.

Moutier, E., Ye, T., Choukrallah, M.-A., Urban, S., Osz, J., Chatagnon, A., Delacroix, L., Langer, D., Rochel, N., Moras, D. et al. (2012). Retinoic acid receptors recognize the mouse genome through binding elements with diverse spacing and topology. *J. Biol. Chem.* **287**, 26328-26341.

Nakai, S., Kawano, H., Yudate, T., Kuno, J., Nagata, A., Jishage, K., Hamada, H., Fujii, H., Kawamura, K. et al. (1995). The POU domain transcription factor Brn-2 is required for the determination of specific neuronal lineages in the hypothalamus of the mouse. *Genes Dev* **9**, 3109-3121.

Niederreither, K. and Dollé, P. (2008). Retinoic acid in development: towards an integrated view. *Nat. Rev. Genet.* **9**, 541-553.

Nieto, L., Joseph, G., Stella, A., Henri, P., Burlet-Schiltz, O., Monsarrat, B., Clottes, E. and Erard, M. (2007). Differential effects of phosphorylation on DNA binding properties of N Oct-3 are dictated by protein/DNA complex structures. *J. Mol. Biol.* **370**, 687-700.

Okabe, S., Forsberg-Nilsson, K., Spiro, A. C., Segal, M. and McKay, R. D. G. (1996). Development of neuronal precursor cells and functional postmitotic neurons from embryonic stem cells in vitro. *Mech. Dev.* **59**, 89-102.

Phillips, K. and Luisi, B. (2000). The virtuoso of versatility: POU proteins that flex to fit. *J. Mol. Biol.* **302**, 1023-1039.

Ramos, C. and Robert, B. (2005). msh/Msx gene family in neural development. *Trends Genet.* **21**, 624-632.

Ryan, A. K. and Rosenfeld, M. G. (1997). POU domain family values: flexibility, partnerships, and developmental codes. *Genes Dev.* **11**, 1207-1225.

Saburi, S., Hester, I., Goodrich, L. and McNeill, H. (2012). Functional interactions between Fat family cadherins in tissue morphogenesis and planar polarity. *Development* **139**, 1806-1820.

Schonemann, M. D., Ryan, A. K., McEvilly, R. J., O'Connell, S. M., Arias, C. A., Kalla, K. A., Li, P., Sawchenko, P. E. and Rosenfeld, M. G. (1995). Development and survival of the endocrine hypothalamus and posterior pituitary gland requires the neuronal POU domain factor Brn-2. *Genes Dev.* **9**, 3122-3135.

Schonemann, M. D., Ryan, A. K., Erkman, L., McEvilly, R. J., Bermingham, J. and Rosenfeld, M. G. (1998). POU domain factors in neural development. *Adv. Exp. Med. Biol.* **449**, 39-53.

Sugitani, Y., Nakai, S., Minowa, O., Nishi, M., Jishage, K., Kawano, H., Mori, K., Ogawa, M. and Noda, T. (2002). Brn-1 and Brn-2 share crucial roles in the production and positioning of mouse neocortical neurons. *Genes Dev.* **16**, 1760-1765.

Tomilin, A., Reményi, A., Lins, K., Bak, H., Leidel, S., Vriend, G., Wilmanns, M. and Schöler, H. R. (2000). Synergism with the coactivator OBF-1 (OCA-B, BOB-1) is mediated by a specific POU dimer configuration. *Cell* **103**, 853-864.

Trapnell, C. and Salzberg, S. L. (2009). How to map billions of short reads onto genomes. *Nat. Biotechnol.* **27**, 455-457.

Trapnell, C., Pachter, L. and Salzberg, S. L. (2009). TopHat: discovering splice junctions with RNA-Seq. *Bioinformatics* **25**, 1105-1111.

Vierbuchen, T., Ostermeier, A., Pang, Z. P., Kokubu, Y., Südhof, T. C. and Wernig, M. (2010). Direct conversion of fibroblasts to functional neurons by defined factors. *Nature* **463**, 1035-1041.

Wapinski, O. L., Vierbuchen, T., Qu, K., Lee, Q. Y., Chanda, S., Fuentes, D. R., Giresi, P. G., Ng, Y. H., Marro, S., Neff, N. F. et al. (2013). Hierarchical mechanisms for direct reprogramming of fibroblasts to neurons. *Cell* **155**, 621-635.

Wichterle, H., Lieberam, I., Porter, J. A. and Jessell, T. M. (2002). Directed differentiation of embryonic stem cells into motor neurons. *Cell* **110**, 385-397.

Yamada, T., Urano-Tashiro, Y., Tanaka, S., Akiyama, H. and Tashiro, F. (2013). Involvement of crosstalk between Oct4 and Meis1a in neural cell fate decision. *PLoS ONE* **8**, e56997.

Zakaria, S., Mao, Y., Kuta, A., Ferreira de Sousa, C., Gaufo, G. O., McNeill, H., Hindges, R., Guthrie, S., Irvine, K. D. and Francis-West, P. H. (2014). Regulation of neuronal migration by dchs1-fat4 planar cell polarity. *Curr. Biol.* **24**, 1620-1627.

Zhang, Y., Liu, T., Meyer, C. A., Eeckhoute, J., Johnson, D. S., Bernstein, B. E., Nussbaum, C., Myers, R. M., Brown, M., Li, W. et al. (2008). Model-based analysis of ChIP-Seq (MACS). *Genome Biol.* **9**, R137.